LA-UR-18-22138
Approved for public release; distribution is unlimited.

Title: The Volumetric Coefficient of Thermal Expansion of PBX 9502

Author(s): Thompson, Darla Graff
Woznick, Caitlin Savanna
DeLuca, Racci

Intended for: Report

Issued: 2018-03-13

The Volumetric Coefficient of Thermal Expansion of PBX 9502

Darla Graff Thompson, Caitlin Woznick, Racci DeLuca
M-7, High Explosives Science and Technology, Los Alamos National Laboratory, MS C920, P.O. Box 1663, Los Alamos, NM, 87545, dkgraff@lanl.gov

Abstract: TATB (1,3,5-triamino-2,4,6-trinitrobenzene) is an insensitive high explosive (IHE) used in plastic-bonded explosives (PBXs) such as PBX 9502. TATB's plate-like crystals have highly anisotropic coefficient of thermal expansion (CTE) values, where the through-plane direction grows about twice as much as the in-plane directions. Compactions of TATB have preferred alignment of crystals, with resulting CTE anisotropy. Additionally, TATB-based compactions exhibit anisotropic irreversible volume expansion (ratchet growth) when thermal cycled to temperatures away from ambient. From a series of measurements on a thermal mechanical analyzer (TMA), the initial thermal ramps away from ambient were used to estimate the volumetric coefficient of thermal expansion of PBX 9502. The TMA measures the change in axial strain of the material as a function of temperature. Starting at ambient, thermal ramps of 1°C per minute were conducted to various endpoint temperatures from -43°C to 173°C on specimens machined from isostatically-pressed hemispheres of PBX 9502. Anisotropy was measured and the volumetric CTE estimated over this temperature range. For ease of use by experimentalists, a 5^{th}-order polynomial was fit to the calculated change in density as a function of temperature. The CTE of neat TATB, PBX 9502, and the Kel-F binder were compared over the given temperature range. At lower temperatures, TATB expands more than PBX 9502 until the melt temperature of Kel-F (80°C), above which the two exhibit similar CTE values.

1.0 Introduction

TATB (1,3,5-triamino-2,4,6-trinitirobenzene) is an insensitive high explosive (IHE) with a plate-like crystal structure used in plastic-bonded explosives (PBXs) such as PBX 9502 [1]. PBX 9502 contains 95 weight% (wt%) TATB and 5 wt% Kel-F as the polymeric binder. The graphitic TATB crystals have highly anisotropic coefficient of thermal expansion (CTE) values [2], differing by as much as a factor of 20 in different directions. The plate-like TATB has been shown to align during compaction [3,4] and to endow the material with anisotropic CTE values [5-7]. TATB compactions, with and without binder, possess properties of irreversible volume expansion, also called ratchet growth [7-13], with TATB texture-related anisotropy as well.

A large quantity of one-dimensional thermal expansion data on LX-17 (92.5 wt% TATB and 7.5 wt% Kel-F), PBX 9502, and TATB has been collected over the past few

years [6, 7, 9-13]. While the main interest and focus of our work [10-12] has been the application of repeated thermal cycles to quantify PBX 9502 ratchet growth, we realized that data from initial thermal ramps could be used to provide experimenters [14-15] and modelers with estimates of the volumetric coefficient of thermal expansion (CTE) of PBX 9502 in the hemispherical geometry. Here, the data are presented and the approximations and assumptions are summarized. The volumetric CTE is used to plot density variations as a function of temperature (ambient as the reference point) and a polynomial fit to the curve is provided. Additionally, a comparison of CTE values for PBX 9502, as-pressed TATB, and the Kel-F binder are also shown and discussed.

2.0 Experimental

One-dimensional thermal expansion measurements were made on a TA Instruments Q400 thermal mechanical analyzer (TMA) which measures the change in strain of a material as a function of temperature. CTE data used here were taken from the initial ramps of PBX 9502 and TATB ratchet growth experiments where specimens were thermal cycled multiple times to various temperatures between -43°C and 173°C [10-13]. An example of TATB data from a full set of thermal cycles is shown in Figure 1. PBX 9502 data is very similar.

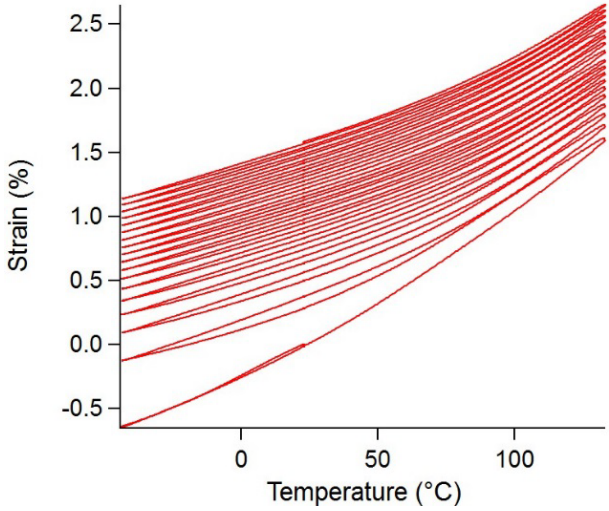

Figure 1: Example of TATB thermal expansion data for TATB thermal cycled 18 times between -43°C and 133°C.

For a linear material, such as aluminum or copper, the expansion data such as that in Figure 1, would move up and down on a single line. Here, for a dry compaction of TATB, the irreversible volume expansion is observed as the data "ratchets" upwards with each thermal cycle. Note, importantly, that the CTE (slope) of the material evolves as the density changes; it tends to be different for increasing versus decreasing temperatures, and is certainly different from one cycle to the next. In order to estimate a volumetric CTE that is useful to experimentalists who want to estimate a specimen density at a test temperature, starting with a known density at ambient, only data from the initial

temperature excursions were used. Specifically, CTE data from 23°C down to -43°C, from -43°C up to 173°C, or from 23°C up to 173°C. All thermal ramp rates were 1°C/min.

PBX 9502 and neat TATB specimens were right cylinders, 5 mm in diameter and 5 mm in length. Specimens this small do not give accurate densities using immersion methods, therefore, densities were obtained manually using measured mass and dimensions. TATB specimens were pressed to shape with an average approximate density of 1.8927 g/cm^3 +/- 0.0002. PBX 9502 specimens were machined from an isostatically-pressed hemisphere and are assumed to have a nominal density of 1.890 g/cm^3 +/- 0.005. TATB texture in PBX 9502 hemispheres have been well-characterized [3, 5, 11], and the texture of the dry-pressed TATB specimens may be somewhat similar. The majority of PBX 9502 cylinders were cut in the radial direction of the hemisphere, with the largest expansion expected in the axial direction.

3.0 Results and Discussion

3.1 Initial Analysis and Factors Effecting Axial CTE Measurements

Figure 2 shows some of the axial CTE expansion data plotted as (a) strain versus temperature, (b) the derivative, or CTE, versus temperature, and (c) a linear approximation of CTE versus temperature. The original strain versus temperature data is very smooth, but the derivative data is noisy and exaggerates small differences. In their work on LX-17 [9], Maienschein and Garcia performed second-order polynomial fits to the strain versus temperature data, then took the derivative of the polynomial. In Figure 2, one can see the simplifying effect on the data, but also that significant detail is lost. In Figure 2(c), we have included Maienschein's axial CTE [9] for an as-pressed cylinder of LX-17 (black line).

Figure 2 includes data from a single transverse-cut specimen (denoted * in the legend) obtained from a different (but similarly-pressed) PBX 9502 hemisphere in a different study [3] as well as data from two of our radial-cut specimens turned on their sides. Note that for the radial specimens tested sideways, the probe force was varied. The probe force is selected by the operator at the outset of the measurement, and is held constant at all temperatures. The force should be large enough to get reproducible data, but small enough that it does not adversely affect the measurement with compressive creep at higher temperatures. The probe force on transverse specimens, shown in Figure 2, does not appear to effect the CTE measurement.

For CTE data in the sub-ambient range, Figure 2, a slight difference is seen in the expansion response of ascending versus descending temperature directions. Figure 2 data confirm the expected TATB texture-based CTE anisotropy. The data in Figure 2 compare very well with the comprehensive CTE dataset reported by Cunningham et al., at LLNL [5], also from isostatically-pressed hemispheres of PBX 9502.

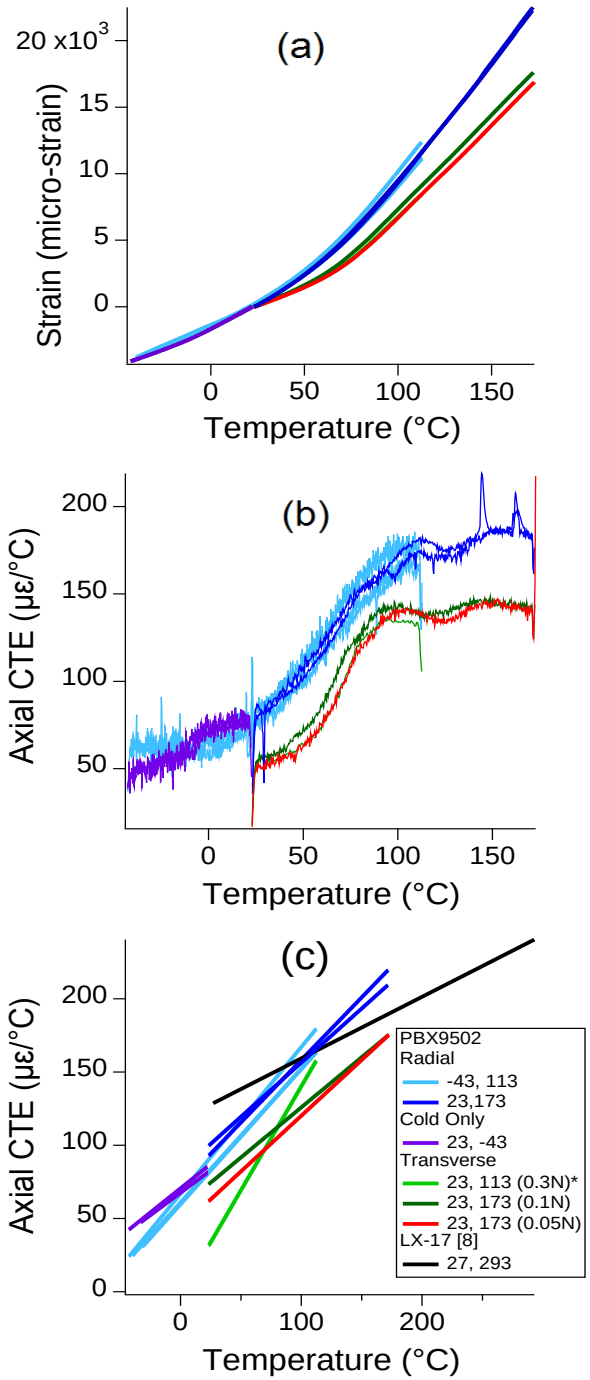

Figure 2: (a) Strain versus temperature, (b) CTE (derivative of raw data) vs. temperature, and (c) CTE (derivative of 2nd order polynomial fits to raw data) versus temperature, all of PBX 9502 in the radial and transverse directions with temperature either ascending or descending. In the legend, first number is the start temperature, second number is the end temperature. LX-17 data from [9] is included.

Figure 3 shows a slightly different subset of PBX 9502 thermal expansion data than that shown in Figures 2. Again, the derivative of the raw strain versus temperature data, Figure 3a, is plotted as 3b. The raw data in Figure 3a were fit with second-order polynomials [9] and are plotted as derivatives of the fit in Figure 3c. All cylindrical specimens in Figure 3 are radial cut from hemispheres, tested axially. We see the effect of probe force as well as thermal history (ascending or descending through the temperature range). A probe force increase from 0.1 to 0.3 to 0.5 N has a decreasing

effect on the measured thermal expansion, especially at high temperature where the material has softened (Kel-F glass transition, Tg, at 28°C). This is due to the compressive creep effect of the probe force. For these data we believe the lighter the probe force the more accurate the CTE. The volumetric CTE calculation will proceed with the blue curves (descending) and the gold curve (ascending) as being the most representative CTE curves of pristine material from 23°C.

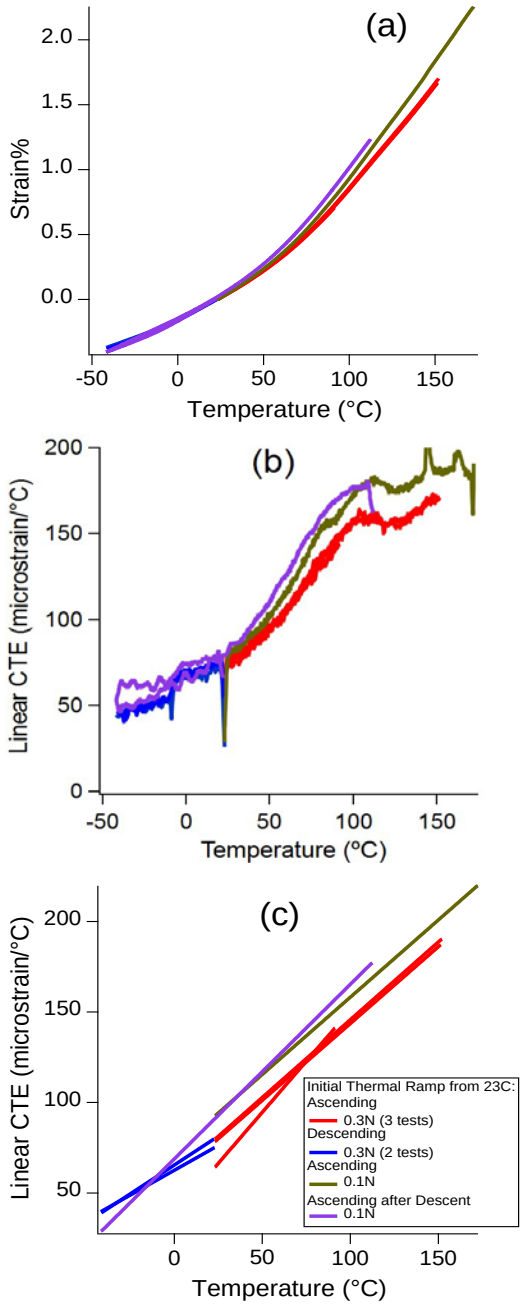

Figure 3: (a) Strain versus temperature, (b) CTE (derivative of raw data) vs. temperature, and (c) CTE (derivative of 2nd order polynomial fits to raw data) versus temperature, of PBX 9502 in the radial direction with temperature either ascending or descending through the temperature range.

3.2 Volumetric CTE of Isostatically-Pressed PBX 9502 Hemispheres

To estimate volumetric CTE we will account for the measured TATB texture [2] and corresponding effect on CTE anisotropy. Only texture data from isostatically-pressed hemispheres of PBX 9502 are considered here. The extent of TATB texturing may be quite different in other pressings.

We define the CTE texture ratio to be the ratio of the CTE measured in the transverse direction versus that measured in the radial direction. In Figure 4, transverse and radial cylindrical specimen axes are shown relevant to the geometry of the hemispherical pressing and preferred TATB orientation. The TATB platelets are aligned with the inner hemispherical surface, and so transverse and radial also define the axes of a three-dimensional ellipsoid that captures the CTE anisotropy.

In Figure 4, the CTE texture ratios of PBX 9502 in the hemispherical geometry are plotted from three different sources. The black circles are taken from the data [10] shown in Figure 2. The red squares are from estimated averages of data in the Cunningham report [5]. The full data set in the Cunningham report clearly shows a significant texture gradient in the radial direction, while the transverse specimens were cut from a single central location. For the purposes of this analysis, we have used the averaged radial and transverse values to calculate the CTE texture ratio in Figure 4. The Cunningham data was measured by lowering the temperature to -55°C and providing CTE data from the ascending thermal ramp.

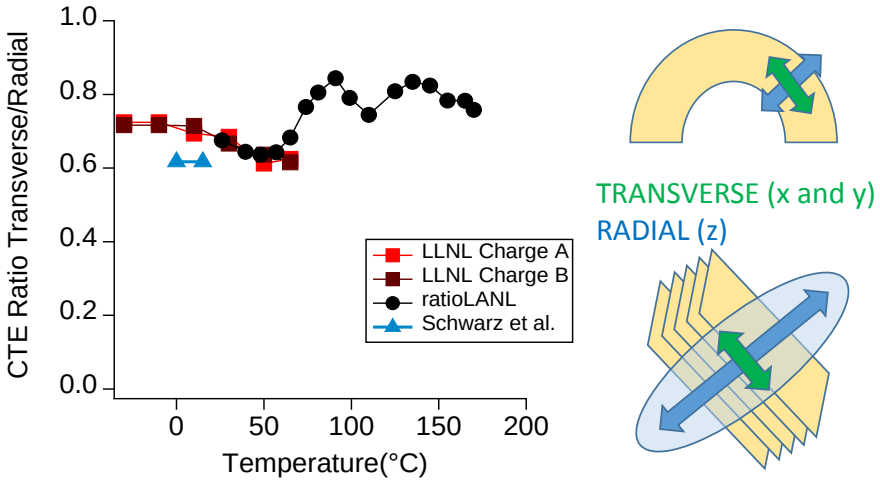

Figure 4: CTE texture ratio versus temperature from three sources; diagrams showing transverse and radial directions relative to hemisphere and the TATB dominant texture.

In Figure 12 of Ricardo Schwarz's work on PBX 9502 texture [10, 11], the CTE anisotropy measured from 0 to 15°C is shown as an ellipse with values of 81, 50 and 50 με/°C. These CTE measurements were made across the diameter of a single disk by rotating the disk in between each linear temperature ramp. To ensure that ratchet growth effects did not contribute to repeated CTE measurements on a single specimen, the

specimen was first subjected to many thermal cycles over a slightly larger temperature range. In Figure 4, this may be the reason the Schwarz data (blue triangles) differ slightly from the others in this temperature region.

The data in Figure 4 suggest that the shape of the CTE ellipsoid (i.e. underlying TATB texture) may change somewhat as a function of temperature and thermal history. The data come from four different PBX 9502 hemispheres, and the Cunningham dataset is extensive, quantifying the CTE variation from inner to outer surfaces of two different hemispheres. For the purposes of our volumetric CTE estimation, we have chosen to simplify the data in Figure 5 by assuming a constant CTE texture ratio of 0.70 over the full temperature range. The calculation of volumetric CTE from axial or linear CTE goes as follows:

$$CTE_{volumetric} = 2 \times CTE_{transverse} + CTE_{radial}.$$

If we assume that

$$CTE_{transverse}/CTE_{radial} = 0.7,$$

then,

$$CTE_{volumetric} = 2.4 \times CTE_{radial}.$$

Using these relationships, volumetric CTE values were calculated from radial CTE values in Figure 3 and they are plotted below as a derivative CTE plot in Figure 5(a) and as linear approximation data in Figure 5(b). Next, we assume that the data in Figure 5 is relatively independent of initial density and is valid for any specimen whose starting density falls within the specification range of 1.890 +/- 0.005 g/cm^3. In Figure 6, a starting density of 1.890 g/cm^3 is assumed and the data is plotted as specimen density versus temperature. For Figure 6, only the curves with the lowest probe force (0.1N) were used, one ascending from ambient and one descending.

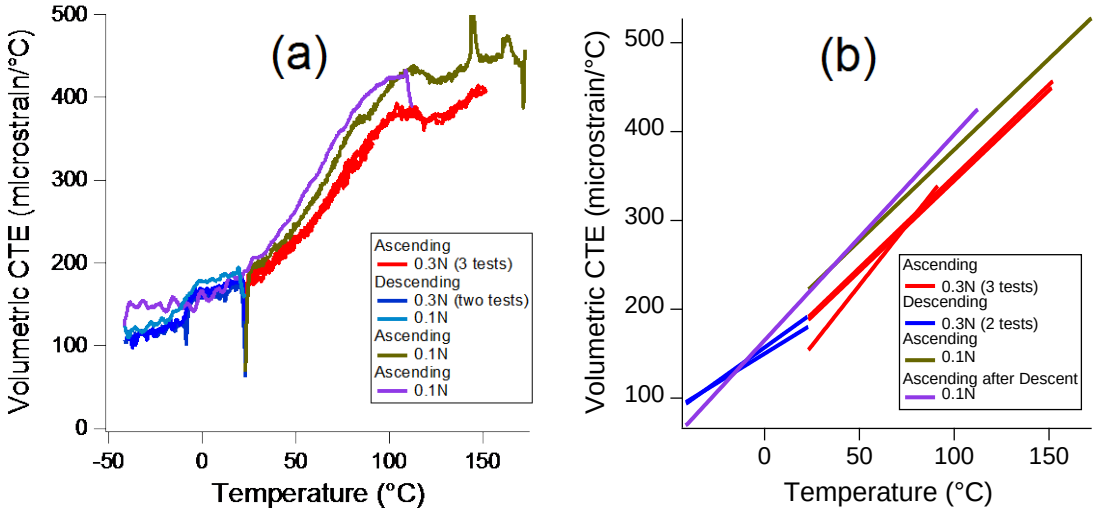

Figure 5: Volumetric CTE plotted versus temperature using the axial CTE data derived from (a) measured data and (b)2nd-order polynomial fits. See text for details.

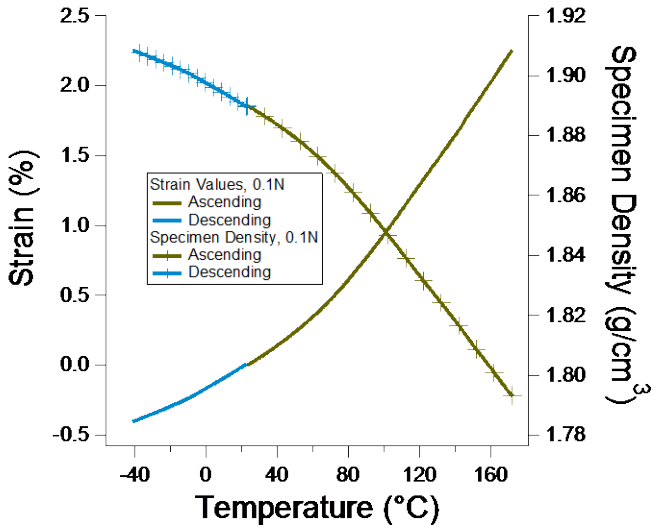

Figure 6: Strain and calculated specimen density (+ symbols)versus temperature assuming a starting density of 1.890 g/cm^3 at 23°C, calculated from volumetric CTE for select curves. See text for details.

Both curves in Figure 6 can be well-represented with a 5th order polynomial equation:

$$y = K_0 + K_1 x + K_2 x^2 + K_3 x^3 + K_4 x^4$$

where the coefficients for the combined density curves are: $K_0 = 1.898$, $K_1 = -0.000286$, $K_2 = -1.067 \times 10^{-6}$, $K_3 = -1.638 \times 10^{-8}$, and $K_4 = 6.839 \times 10^{-11}$ and the coefficients for the combined strain curves are: $K_0 = -0.167$, $K_1 = 0.062$, $K_2 = 2.385 \times 10^{-5}$, $K_3 = 3.883 \times 10^{-7}$, and $K_4 = -1.531 \times 10^{-9}$.

The estimates made in Figure 5 and 6 are for PBX 9502 specimens taken from isostatically-pressed hemispheres at nominal density as described above. It is possible that axially die-pressed cylinders may have a dominant TATB orientation in some ways similar to that of an isostatically-pressed hemisphere [6, 15], and that the data in Figure 5 and 6 can be extended to that geometry as well, but caution is warranted. The TATB texturing of die-pressed PBX 9502 parts is likely complicated by interaction with the die walls, and therefore die-pressed cylinders likely have an inner-to-outer texture gradient far more complex than what is found in cylinders machined from hemispheres. Preliminary volumetric CTE measurements on specimens machined from the center of large die-pressed PBX 9502 cylinders (l/d=1) suggest that the overall TATB texture and CTE anisotropy may be quite different from the measured in PBX 9502 hemispheres. Caution should be used in the extrapolation of data from Figures 5 and 6 to any other pressed geometries [6, 9].

3.3 Comparison of Axial CTE of PBX 9502, TATB, and Kel-F

Figure 7 shows changes in strain from -43°C to 113°C for neat TATB, PBX 9502, and Kel-F. The Kel-F data stops at 80°C because the polymer melts at that temperature. The Kel-F glass transition (T_g) at 28°C can be seen as a discontinuity in Figure 7. The PBX 9502 data is from the radial direction, described above, while the TATB specimens were as-pressed cylinders. The dominant orientation of the TATB texture for the PBX 9502 and TATB specimens may be somewhat similar, although the relative texture distribution/magnitude of the TATB is not known. The CTE curves are different for all three materials at low temperatures and come together near ambient. Just above ambient (and the Kel-F T_g), the PBX 9502 grows less than the TATB; more measurements will distinguish if growth is actually restricted in the PBX or if this is a compressive creep effect caused by the probe force on the softening binder. The Kel-F CTE follows the PBX 9502 curve above ambient showing that the polymer and PBX have similar growth in this temperature region.

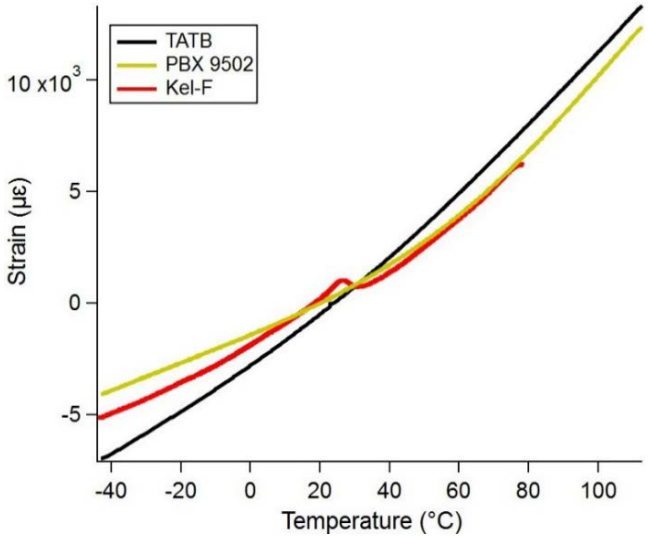

Figure 7: Strain vs. temperature of neat TATB, PBX 9502, and Kel-F.

Figure 8 shows the CTE from -43°C to 173°C of the neat TATB, PBX 9502, and Kel-F using (a) the derivative of the measured data, and (b) and the second-order polynomial fits [9]. The Kel-F in Figure 8(b) is plotted as two lines on either side of the T_g. The CTE from 23°C to -43°C (descending temperature) is shown for TATB (dark blue) and for PBX 9502 (purple) in Figure 8. For both materials, the ascending versus descending CTE between -43 and 23°C is very different. As mentioned previously, this difference is due to the effect of thermal history and ratchet growth.

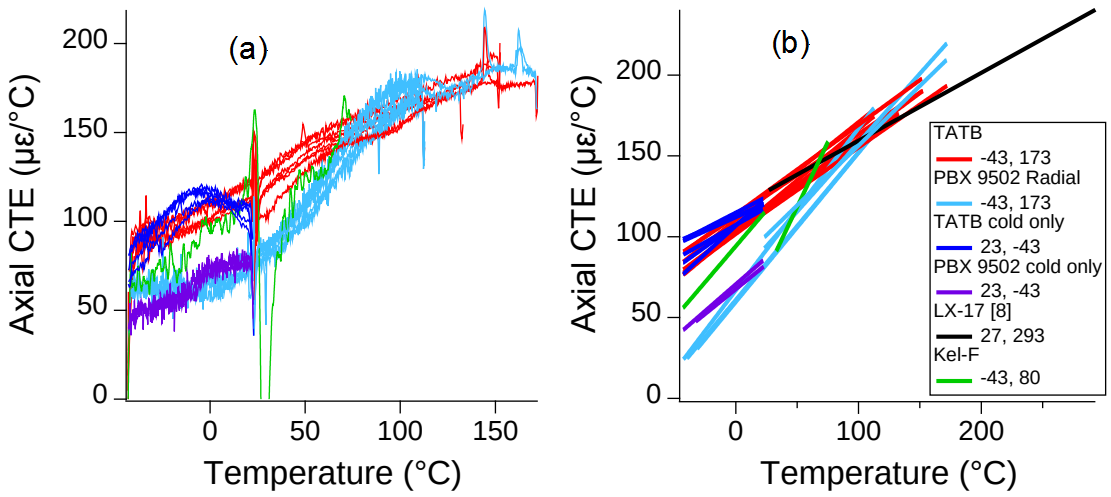

Figure 8: CTE vs. temperature of neat TATB, PBX 9502, and Kel-F. In the legend, first number listed is the start temperature, second number is the stop temperature of the TMA measurement. CTE derived from (a) real data and (b) 2nd-order polynomial fit data.

4.0 Conclusions

The volumetric CTE of PBX 9502 has been estimated for isostatically-pressed hemispheres. This includes measurements and assumptions about TATB texture effects for this geometry, and the data are also plotted as specimen density versus temperature from a starting point of 1.890 g/cm^3 at 23°C. In the CTE measurements, initial temperature excursions from ambient were used in order to avoid complications of thermal history and ratchet growth. Additionally, the lowest probe force was used to minimize compressive creep. The axial CTE of PBX 9502 and its constituents are also shown, although textures may differ in the PBX 9502 and TATB specimens. Above the Kel-F melt temperature, the axial PBX 9502 CTE approaches that of the die-pressed TATB cylinders.

Acknowledgements

We thank the M-7 Pressing Team, Laida Valdez in particular, for pressing the dry TATB powder specimens. This work was supported by the U.S. Department of Energy through the Los Alamos National Laboratory. Los Alamos National Laboratory is operated by Los Alamos National Security, LLC, for the National Nuclear Security Administration of U.S. Department of Energy (Contract DEAC52-06NA25396).

References

[1] “The Insensitive High Explosive Triaminotrinitrobenzene (TATB): Development and Characterization – 1888 to 1994,” Dobratz, B.M., Los Alamos National Laboratory, August **1995**, Report *LA-13014-H*.

[2] “Growth of 1,3,5-Triamino-2,4,6-trinitrobenzene (TATB) I. Anisotropic Thermal Expansion, Kolb, J.R., Rizzo, H. F., *Propellants and Explosives,* **1979,** *4*, 10-16.

[3] “The Effect of Shear Strain on Texture in Pressed Plastic Bonded Explosives,” Schwarz, R., Brown, G.W., Thompson, D.G., Olinger, B.W., Furmanski, J., Cady, H.H., *Prop. Expl. Pyrotech.*, **2013**, *38*, 685-694.

[4] “Neutron Diffraction Measurements and Micromechanical Modelling of Temperature-Dependent Variations in TATB Lattice Parameters,” Yeager, J.D., Luscher, D.J., Vogel, S.C., Clausen, B., Brown, D.W., *Prop. Expl. Pyrotech.*, **2016**, *41*, 514-525.

[5] “Thermal Expansion Measurements on Samples Cored from Hemispherical Pressings,” Cunningham, B., Andreski, H., Weese, R., Turner, H., Lauderbach, L., Lawrence Livermore National Laboratory, 11 April **2005**, informal report on HEAF Mechanical Properties.

[6] “The Elusive Coefficients of Thermal Expansion in PBX 9502,” Skidmore, C.B., Butler, T.A., Sandoval, C.W., January 2003, LA-14003.

[7] Unpublished results, Cady, H.H., Los Alamos National Laboratory.

[8] “Growth of 1,3,5-Triamino-2,4,6-Trinitrobenzene (TATB), Control of Growth by Use of High Tg Polymeric Binders,” Rizzo, H.F., Humphrey, J.R., Kolb, J.R., Lawrence Livermore National Laboratory, **1979**, Report *UCRL-52662*.

[9] “Thermal Expansion of TATB-Based Explosives from 300 to 566 K,” Maienshein, J.L., Garcia, F., *Thermochimica Acta*, **2002**, *384*, 71-83.

[10] “Characterization of PBX 9502 Ratchet Growth in Hemispherical Pressings,” Thompson, D.G., DeLuca, R., Los Alamos National Laboratory, 27 April **2017**, internal report, *LA-UR 17-23650*.

[11] “Anisotropy in Ratchet Growth of PBX 9502,” Schwarz, R.B., Liu, C., Thompson, D.G., Los Alamos National Laboratory, 12 March **2015,** internal report, *LA-UR-15-21827*.

[12] “Time Evolution of TATB-Based Irreversible Thermal Expansion (Ratchet Growth),” Thompson, D.G., Schwarz, R.B., Brown, G.W., DeLuca, R., *Prop. Expl. Pyrotech.*, **2015**, *40*, 558-565.

[13] “Thermal Cycling and Ratchet Growth of As-Pressed TATB Pellets,” Woznick, C.S., Thompson, D.G., DeLuca, R., Patterson, B., Shear, T.R., Proceedings of the APS-SCCM, St. Louis, MO, July **2017**, *LA-UR-17-27817*.

[14] “The reactants equation of state for the triaminotrinitrobenzene (TATB) based explosive PBX 9502,” Aslam, T.D., *J. Appl. Phys.*, **2017**, 122(3), 035902, *LA-UR-17-24446*.

[15] Unpublished results, Crane, C., Adams, A., et al., Los Alamos National Laboratory, **2017**.